Stochastic inversion of pressure and saturation changes from time-lapse seismic data.

Helene Hafslund Veire[(1)], Hilde Grude Borgos[(2)], Martin Landrø[(1)], [(1)] Norwegian University of Science and Technology, [(2)] Schlumberger Stavanger Research.*

Summary

The effects of pressure and fluid saturation can have the same degree of impact on seismic data, thus they are often inseparable by analysis of a single seismic data set. In such cases the use of time lapse AVO analysis offers an opportunity to discriminate the two effects.

To be able to utilize the information about pressure and saturation related changes in reservoir modelling and simulation, we need to quantify the uncertainty in the estimations. One way of analysing the uncertainties is by formulating the problem in a Bayesian framework. Here, the solution of the problem will be represented by a probability density function, giving us an immediate view for the uncertainty in the estimations.

In this paper a stochastic model for estimation of pressure and saturation changes from time-lapse seismic data has been investigated within a Bayesian framework. The formulation of the relationship between time-lapse AVO data and pressure and saturation changes has been based on the works of Landrø (1999 and 2001). Well-known rock physical relationships have been used to set up a prior stochastic model. Shuey's linearization of Zoeppritz' equations for the PP reflection coefficient has been used to estiablish a likelihood model for linking the reservoir variables and the time-lapse seismic data.

The methodology has been tested out on 1D synthetic data and on time-lapse seismic AVO data from the Gullfaks Field in the North Sea.

Introduction

The traditional way of predicting overpressured zones from seismic data has been through velocity analysis, by detecting areas where the velocities estimated from seismic data deviated from the normal trend. Fluid effects are often analysed by investigating AVO effects on the PP seismic data, e.g. Castagna et al. (1994).

However, it is often difficult to separate the effects of pressure and fluid saturation from a single set of seismic data alone. In some cases saturation and pressure changes have approximately the same degree of impact on stacked seismic data. In such cases the use of time lapse AVO analysis offers an opportunity to discriminate the two effects (Tura and Lumley, 1999, Landrø, 2001).

To be able to utilize the information about pressure and saturation related changes in reservoir modelling and simulation, we need to quantify the uncertainty in the estimations. Landrø (2002) presented a deterministic analysis of uncertainty in the estimation of pressure and saturation changes from time-lapse AVO-data and traveltime differences, assuming independent variables in the calculations. Incorporation of the correlation between the different variables can be done by formulating the problem in a Bayesian framework. Here, the solution of the problem will be represented by a probability density function, giving us immediate information of the uncertainty in the estimations. One additional advantage of the stochastic representation is the possibility to include spatial correlation in the estimation of the variables.

Theoretical relationships may be linked to measured data through a stochastic framework, by representing the theoretical relationships in an a priori probability distribution, and letting a likelihood model describe the degree of fit between the measured data and data predicted from the models. The posterior probability can then be found by applying Bayes rule. Other examples of how different types of geophysical and well log data have been integrated in a stochastic framework to estimate various properties of the subsurface can be found in e.g. Malinverno and Leaney (2000), and Eidsvik et al. (2002).

In the following, a stochastic model to estimate fluid and pressure related changes directly from repeated pressure wave offset data will be presented. The methodology has been tested on synthetic seismic data and real data from the Gullfaks Field in the North Sea.

Methodology

Through well known rock physical relationships, links between the measured seismic variables (*Dt, Dr0, Dg*) and the reservoir parameters *DSw* and *DP* are set up. Here, *Dt* represents the time-lapse change in travel time over the reservoir interval, (*Dr0, Dg*) are the time-lapse change in AVO intercept and gradient, and *DSw* and *DP* are the change in saturation and pressure due to production.

The prior model connecting the production related change in elastic parameters with the change in seismic parameters (travel time change and change in P-wave velocity, S-wave velocity and density) is defined by combining well-known rock physical relationships. These relationships give the expectance value for the prior distributions. Gaussian errors are added to the expectance values, giving Gaussian prior distributions.

The relationship between relative change in P-wave velocity and relative change in travel time due to production is based on differentiating the basic relationship between zero offset interval traveltime, thickness of layer, and P-wave velocity, given by $t=2Z/a$, where t is the zero offset interval traveltime, Z is the thickness of the layer, and a is the P-wave velocity. In the prior distribution of the relative change in P-wave velocity, the change in travel time, *Dt*, is treated as an exact observation. In future work, a mixed Gaussian model can be used as a prior model for the travel time change.

The change in saturation as a function of density can be derived from the relationship between density, porosity and saturation

$$r = (1-f)\cdot r_M + f\cdot\left[Sw\cdot r_W + (1-Sw)\cdot r_{HC}\right] \qquad (1)$$

Here, r is the bulk density, r_M is the matrix density, r_{HC} is the oil density, r_W is the water density, f is the porosity, and *Sw* is the water saturation.

The change in P-wave velocity can be separated into a saturation-related change and a pressure related change. By differentiating Gassmanns equation with respect to velocity, density and fluid modulus, we get an expression for the change in P-wave velocity as a function of change in density and fluid modulus. The change in P-wave velocity as a function of change in pressure can be derived from a modified version of the Hertz-Mindlin model for normal compression of identical spheres as suggested by Vidal et al. (2002).

The change in S-wave velocity due to production depends on the change in saturation through the change in density, and the change in pressure through the shear modulus given by the modified Hertz-Mindlin model.

In addition, a prior distribution for the change in saturation given the relative change in P-wave velocity is needed. We assume that half the change in velocity is due to a change in pressure, adding onto this a large variance, making the prior distribution very wide.

The prior probability density function (pdf) of the reservoir variables (r) will then be on the form

$$f(r) = f(\Delta Sw, \Delta P, \frac{\Delta a}{a}, \frac{\Delta b}{b}, \frac{\Delta r}{r}) = f(\frac{\Delta a}{a})\cdot f(\Delta Sw \mid \frac{\Delta a}{a})\cdot f(\frac{\Delta r}{r} \mid \Delta Sw)\cdot f(\Delta P \mid \frac{\Delta a}{a}, \Delta Sw)\cdot f(\frac{\Delta b}{b} \mid \Delta P, \frac{\Delta r}{r}) \qquad (2)$$

Here, *f(Da/a)* is the pdf of the relative change in P-wave velocity, *f(DSw|Da/a)* is the prior pdf of the change in water saturation given the relatve change in P-wave velocity, *f(Dr/r|DSw)* is the prior pdf of the relative change in density given the change in saturation, *f(DP|Da/a,DSw)* is the prior pdf of the change in pressure given the change in saturation and the relative change in P-wave velocity, and *f(Db/b|DP, Dr/r)* is the prior pdf of the relative change in S-wave velocity given the change in pressure and the relative change in density.

The likelihood model for the seismic data describes how the relative change in the seismic parameters P-wave velocity, S-wave velocity and density are related to the measured change in the seismic amplitudes. We are using the formulation from Landrø (2001), where the change in AVO intercept and gradient for 4D PP seismic data is given by a relative change in density, P-wave velocity and S-wave velocity.

The posterior model can be found from

$$f(r \mid \Delta r0, \Delta g) = C\cdot f(\Delta r0, \Delta g \mid r)\cdot f(r), \qquad (3)$$

where C is the normalizing, and *f (Dr0, Dg|r)* is the likelihood model. By inserting the expressions from the prior model, we get the following expression for the posterior model:

$$f(r \mid \Delta r0, \Delta g) \propto f(\Delta r0, \Delta g \mid r)\cdot f(\frac{\Delta a}{a})\cdot f(\Delta Sw \mid \frac{\Delta a}{a})\cdot f(\frac{\Delta r}{r} \mid \Delta Sw)\cdot f(\Delta P \mid \frac{\Delta a}{a}, \Delta Sw)\cdot f(\frac{\Delta b}{b} \mid \Delta P, \frac{\Delta r}{r}) \qquad (4)$$

Since all the factors of the prior and likelihood model are Gaussian distributions, and the expectations are linear relationships, the posterior distribution will also be a Gaussian distribution, and thus analytically tractable.

Examples

Three-layer synthetic models with properties taken from a well in the Gullfaks Field were built. The rock physical properties of the cap rock layer and the layer below the reservoir zone were kept constant, and only the parameters of the reservoir rock were perturbed. The relationship between the seismic parameters and pressure was found through statistical analysis of ultrasonic measurements from dry cores of various formations. The seismic parameters for different scenarios for saturated reservoir rock were calculated using Gassmann’s equation.

From the synthetic reservoir models, reflection coefficients were calculated using Zoeppritz’ equations for angles of incidence from 0 to 20 degrees, and the reflection coefficients were convolved with a 30Hz Ricker wavelet. Pairs of two models representing pre- and post-production stages were analysed to estimate the pressure and saturation changes from the seismic data. From the measured difference in zero offset traveltime in the reservoir zone and from differences in AVO intercept and gradient along the top of the reservoir, the parameters for the posterior Gaussian distribution were estimated. The trend model and the prior uncertainties for the P-wave velocity, S-wave velocity, density, water saturation, and pressure were found by statistical analysis of well-log and core data from the

Gullfaks Field, and were equal for all the cases. This implies that the covariance matrix for the Gaussian distribution was the same for all cases. The measured change in AVO intercept and gradient and the change in traveltime thickness for the reservoir zone were influencing the expectance value of the Gaussian distribution. The best results were produced for a relative large change in both water saturation and pressure, see Table 1. The prior model did not handle pressure decreases or no change in pressure well. However, the results lie within one standard deviation of the exact changes for all the cases, showing that the uncertainties of the estimations were large. The correlation matrix between the different variables in the synthetic test is shown in Table 2. Note the large correlation between change in pressure and relative change in S-wave velocity, and between relative change in density and the change in saturation.

The Gullfaks Field is situated in the eastern part of a major NNE-trending fault block in the Tampen Spur area of the North Sea. The reservoir sands are of early and middle Jurassic age, with shallow marine to fluvial deposits. The Gullfaks time-lapse study have been presented by e.g. Landrø et al. (1999b), and Sønneland et al. (1997), and the main objective of the study has been to identify potentially undrained reservoir compartements (Landrø et al, 1999b).

In this study we have used the seismic data acquired in 1996 and in 1999. The two datasets have almost the same acquisition configuration. The processing of the two seismic surveys follows a standard processing sequence, and was kept as similar as possible between the two surveys. No cross-equalization was done on the data.

The method requires as input a trend model, in addition to the difference in two-way travel time reservoir thickness, the time-lapse change in AVO intercept and gradient. We have used the near-, mid-, and far offset partial stacks, with identical offset ranges for the two seismic vintages to estimate the AVO parameters for the reservoir interval. The difference in two way traveltime thickness was found on the full stack dataset, by interpreting the base of the reservoir interval on both the 1996 and 1999 datasets (assuming no change along the top of the reservoir) and taking the difference. Integrated reflection strength volume attributes were generated over the reservoir interval on the three offset cubes for both the 1996 and 1999 data. The attribute grids were calibrated to reflection coefficients by using a trend model built from well log data for velocity and density. The same calibration factor was used for the three offset cubes from both the seismic vintages. The AVO gradient was constructed by fitting a line to the calibrated attributes for near-, mid-, and far-offsets. Finally difference grids were calculated for the AVO intercept and gradient.

The covariance matrix of the prior distribution was estimated from a trend model, and defined to be spatially invariant. The standard deviation of the change in saturation was about 0.77, and the standard deviation in the change in pressure was about 4.5 MPa. The expectance values for the 5 dimensional Gaussian distribution were calculated from the data. In addition to the correlation between the different parameters, as set up in the prior model, spatial correlation was included. Figure 1 shows the expectance value for the time-lapse saturation change (above) and one realization of saturation change with an exponential correlation model and a correlation length of 25 m. Figure 2 show the expectance value (top) for the change in pressure, and the corresponding realization of pressure change (bottom) with the same parameters as the saturation maps. The simulations will have a larger value range (+/- two standard deviations) than the expectance values. The time lapse seismic input grids (change in travel time thickness of the reservoir, and change in AVO attributes) did not show clear and continuous changes, and this will be reflected in the estimated change in pressure and saturation. However, we do observe trends that correlate with information about water injection in Well 1 (Figure 1 and 2) in this area.

Conclusions

The method has been tested on synthetic data and on time-lapse seismic AVO data from the Gullfaks Field in the North Sea. Both synthetic and real tests show that there are large uncertainties in the estimation of pressure and saturation changes from seismic data. The strong correlation between change in pressure and change in S-wave velocity indicates that information about S-wave velocities is essential to obtain good estimates of pressure.

The methodology presented in this paper allows us to estimate pressure and saturation changes from time lapse AVO data, giving as additional information the uncertainty in the estimations. The methodology incorporates correlation between the different variables of the models, as well as spatial correlation for each of the variables. In addition, information about possible bottlenecks causing large uncertainties in the estimations can be identified through sensitivity analysis of the system.

References

Castagna, J.P., and Smith, S.W., 1994, Comparison of AVO indicators: A modeling study: Geophysics, **59**, 1849-1855.

Eidsvik, J., Avseth, P., Omre, H., Mukerji, T., and Mavko, G., 2002, Stochastic reservoir characterization using Bayesian integration of rock physics and Markov random fields: A North Sea example: The Leading Edge.

Landrø, M., Solheim, O.A., Hilde, E., Ekren, B.O., and Strønen, L.K., 1999, The Gullfaks 4D seismic study: Petroleum Geoscience, **5**, 213-226.

Landrø, M., 2001, Discrimination between pressure and fluid saturation changes from time-lapse seismic data: Geophysics, **66**, 836-844.

Landrø, M., 2002, Uncertainties in quantitative time-lapse seismic analysis: Geophysical Prospecting, **50**, 527-538.

Malinverno, A., and Leaney, S., 2000, A Monte Carlo Method to quantify uncertainty in the inversion of zero-offset VSP data: 70th Ann. Internat. Mtg., Soc.Explor., Geophys., Expanded Abstracts, 2393-2396.

Shuey, R.T., 1985, A simplification of the Zoeppritz equations: Geophysics, **50**, 609-614.

Sønneland, L., Veire, H.H., Raymond, B., Signer, C., Pedersen, L., Ryan, S., Sayers, C., 1997, Seismic reservoir monitoring on Gullfaks: The Leading Edge, **16**, 1247-1252.

Tura, A. and Lumley, D.E., 1999, Estimating pressure and saturation changes from time-lapse AVO data: 69th Ann. Internat. Mtg., Soc.Explor., Geophys., Expanded Abstracts, 1655-1658.

Vidal, S., Huguet, F., and Mechler, P., 2002, Characterizing reservoir parameters by integrating seismic monitoring and geomechanics: The Leading Edge.

Acknowledgments

We acknowledge the VISTA/Statoil research programme for financial support, and we thank Statoil and their lincense partners, Norsk Hydro and Petoro, for permission to publish data from the Gullfaks Field. We thank Geir Våland Dahl for valuable discussions.

Figures and tables

Sw1/Sw2	P1/P2 (MPa)	Sw diff	P diff (MPa)	Est. Sw diff (st.dev.)	Est P diff (st.dev.) (MPa)
0.1/0.9	2/6	0.8	4	1.04 (0.67)	4.11 (3.30)
0.1/0.5	2/8	0.4	6	0.80 (0.67)	3.20 (3.30)
0.1/0.6	2/6	0.5	4	0.74 (0.67)	2.94 (3.30)
0.5/0.9	8/6	0.4	-2	0.24 (0.67)	0.90 (3.30)
0.6/0.9	6/6	0.3	0	0.30 (0.67)	1.16 (3.30)
0.5/0.6	8/6	0.1	-2	-0.06 (0.67)	-0.26(3.30)

Table 1: Results, synthetic tests. Sw1/Sw2 and P1/P2 are the saturation and pressure before and after production.

	Da/a	Db/b	Dr/r	DSw	DP
Da/a	1	0.33	0.33	0.39	0.41
Db/b	0.33	1	-0.37	0.84	-0.40
Dr/r	0.33	-0.37	1	-0.42	0.83
DSw	0.39	0.84	-0.42	1	-0.48
DP	0.41	-0.40	0.83	-0.48	1

Table 2: Correlation matrix for synthetic tests.

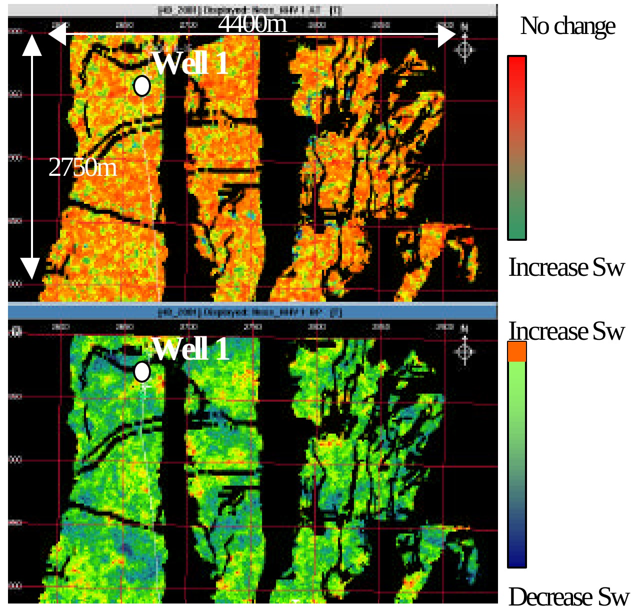

Figure 1: Estimated difference in saturation, expectance value (above) and a realization with spatial correlation (below).

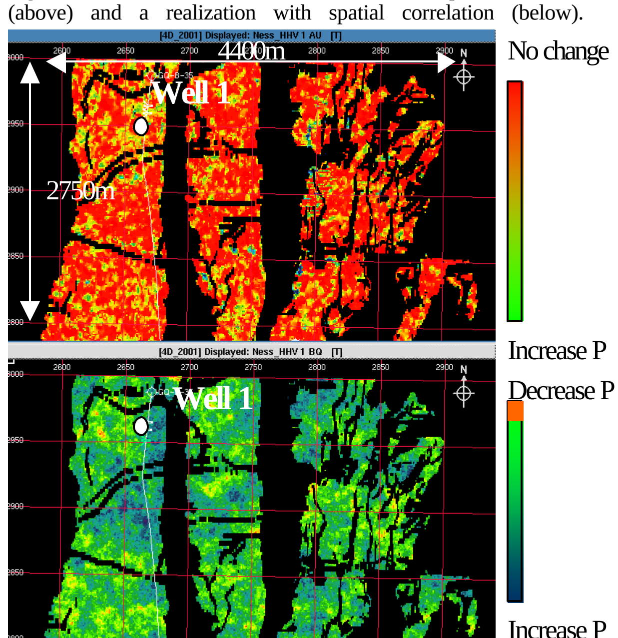

Figure 2: Estimated difference in pressure, expectance value (above) and a realization with spatial correlation (below)